

The convergence of the ab-initio many-body expansion for the cohesive energy of solid mercury

Beate Paulus, Krzysztof Rosciszewski*

Max-Planck-Institut für Physik komplexer Systeme,
Nöthnitzer Straße 38, D-01187 Dresden, Germany

* Institute of Physics, Jagellonian University,
Reymonta 4, PL 30-059 Krakow, Poland

Nicola Gaston, Peter Schwerdtfeger

Theoretical Chemistry, Institute of Fundamental Sciences, Massey University (Albany Campus),
Private Bag 102904, North Shore MSC, Auckland, New Zealand

Hermann Stoll

Institut für Theoretische Chemie, Universität Stuttgart,
D-70550 Stuttgart, Germany

A many-body expansion for mercury clusters of the form

$$E = \sum_{i < j} \Delta\epsilon_{ij} + \sum_{i < j < k} \Delta\epsilon_{ijk} + \dots , \quad (1)$$

does not converge smoothly with increasing cluster size towards the solid state. Even for smaller cluster sizes (up to $n=6$), where van der Waals forces still dominate, one observes bad convergence behaviour. For solid mercury the convergence of the many-body expansion can dramatically be improved by an incremental procedure within an embedded cluster approach. Here one adds the coupled cluster many-body electron correlation contributions of the embedded cluster to the bulk HF energy. In this way we obtain a cohesive energy (not corrected for zero-point vibration) of 0.79 eV in perfect agreement with the experimental value.

I. INTRODUCTION

It is nowadays possible to calculate properties from first principles for a wide range of materials. This is mainly due to the success of density-functional theory (DFT)¹. Although the exact exchange-correlation functional is not known, useful approximations are available, the most widespread ones being the local-density approximation (LDA)² and the generalized gradient approximation (GGA)³. While DFT methods perform very well in a wide range of bonding situations (metallic, covalent, ionic), both LDA and GGA have serious problems describing weakly bound systems such as van der

Waals (vdW) crystals⁴. Here, an alternative is to invoke wavefunction-based ab-initio methods of quantum chemistry^{5,6}. These methods allow for a proper account of the vdW interaction in small clusters of atoms (dimers, trimers, ...), and, inserting these data into a many-body expansion of the bulk cohesive energy, it is possible to extract from them reliable results for rare-gas crystals⁷.

Mercury is a special case: starting from the vdW bound dimer (dissociation energy: 0.05 eV⁸), there is a smooth transition from vdW clusters (up to about 20 atoms) to covalent clusters and to the metallic system (more than 400 atoms)^{9,10}, finally leading to the metallic solid with its overlapping *sp* bands (cohesive energy per atom: 0.79 eV¹¹). Whereas the weakly bound dimer can only be reliably described with highly correlated wavefunction-based methods (like the coupled-cluster (CC) approach) and extended correlation consistent atomic basis sets¹²⁻¹⁴, one would expect that the metallic solid should be well described within DFT. Unfortunately, this seems to be not the case: various functionals yield very different results^{15,16}, from overbinding (by 30% with LDA) to severe underbinding (by a factor of nearly 3 with typical GGA functionals like PBE). Mixing in Hartree-Fock (HF) contributions to form hybrid functionals like B3LYP does not help either: with pure HF, the crystal energy at the equilibrium lattice constant is repulsive by about the same magnitude as the experimental value is attractive¹⁷; the binding is entirely due to electron correlation. On the other hand, it may not be surprising that a many-body expansion derived from wavefunction-based correlated cluster data (dimers,

trimers, ...) is of rather limited success also¹⁵, since the metallic bonding of the solid has not much in common with the vdW like behaviour of the smaller clusters. In order to make such an expansion work, it is necessary to introduce solid-state information from the outset.

An attempt into this direction has been made very recently by two of us¹⁷. A method has been proposed for solid mercury, where the mean-field (Hartree-Fock) part is calculated for the infinite solid and only the correlation part is determined within a many-body expansion using the wavefunction-based CC approach; moreover, the CC calculations have been performed for finite, but embedded clusters which mimic the confinement of the electrons in the solid. This way, very good agreement with the experimental cohesive energy has been obtained. In the present paper, we discuss this method in detail, and we compare it with other variants of many-body expansions, with and without embedding, to discuss the convergence behaviour. In the next section (Sec. II) we present our HF calculations. In Sec. III we discuss different possible ways of setting up the many-body expansion. In Sec. IV we construct the embedding. After that (Secs. V to VIII) the individual contributions to the various many-body expansions are presented. From these, the cohesive energy of mercury is evaluated in Sec. IX, and conclusions follow in Sec. X.

II. PERIODIC HARTREE-FOCK

For calculating the HF contribution to the binding in bulk Hg (rhombohedral structure, with equilibrium lattice constant $a_0 = 3.005 \text{ \AA}$ and $\alpha = 70.53^{\circ}$ ¹¹), we use the program package CRYSTAL98¹⁸. We changed the default parameters in order to obtain a converged result for the HF binding energy, i.e. we set integral thresholds to $\leq 10^{-8} \text{ a.u.}$ and convergence criteria for the total energy and the orbital coefficients to 10^{-6} a.u. and 10^{-5} a.u. , respectively; our k -mesh involved 9825 k -points in a Gilat net. The chemically inactive [Kr]4d¹⁰4f¹⁴ core of the Hg atom is simulated by an energy-consistent scalar-relativistic pseudopotential (PP)¹⁹. In CRYSTAL98, the Bloch functions of the solid are generated using local Gaussian-type (GTO) basis functions. In principle, GTO sets optimized for atoms could be used; however, diffuse functions describing atomic tails are not necessary in the densely packed solid (and would in fact lead to convergence difficulties in the SCF procedure if used nevertheless). In our calculations we start from a (7s7p6d1f) set of primitive Gaussians¹⁴; we leave out the most diffuse s and p function and partially reoptimize the next inner ones for the crystal (the resulting exponential parameters are 0.126 for both s and p); we next form fixed linear combinations (contractions) of the first three s and p Gaussians and of the first four d Gaussians using the 5s, 5p, 5d, and 6s atomic orbitals as contraction coefficients; finally, we leave out the f polarization function because

such functions are not too important for the HF cohesive energy of metals without an open d -shell. The resulting contracted GTO (CGTO) basis set can be characterized as (6s6p6d)/[5s4p3d]. In order to provide an *a-posteriori* justification for the truncation of the original atomic basis set, we performed a free-atom calculation with the modified (crystal) basis centered at the site of the atom *and* at the 12 neighbouring atomic positions of the solid. The resulting atomic HF energy is only about 1 mHartree higher than that obtained in a standard free-atom calculation with the original uncontracted (7s7p6d1f) basis set, so that we can use the former value as a reference for calculating the cohesive energy of the solid.

The calculated HF cohesive energy (binding energy per atom) of solid mercury in the rhombohedral structure is listed in Table III. It is seen that there is no binding at the HF level, at least not at the experimental lattice constant of the crystal, in spite of the metallic behaviour signalled by the overlap of the bands derived from the 6s and 6p atomic orbitals; the HF repulsion is of about the same magnitude as the experimental value of the cohesive energy. There is no binding either at the HF level for the dimer Hg₂²⁰, and most likely for all Hg_n clusters up to the solid state. This situation is usually found for vdW systems only.

III. MANY-BODY EXPANSIONS

When setting up a many-body expansion of the form

$$E = \sum_i \epsilon_i + \sum_{i < j} \Delta\epsilon_{ij} + \sum_{i < j < k} \Delta\epsilon_{ijk} + \dots , \quad (2)$$

for the crystal energy (or part of it), one first has to specify the meaning of the n -body indices i, j, k, \dots . Both for a vdW crystal and a metal, a numbering in terms of atoms seems to be natural. However, only if local interactions prevail will n -body contributions for distant atom pairs i, j , triples i, j, k , etc. decay fast enough to make such an expansion useful.

In its simplest form, E is the total crystal energy, the ϵ_i are taken as the (total) energies of the free atoms, the $\Delta\epsilon_{ij}$ are the non-additive parts of the total energies ϵ_{ij} for (isolated) pairs of atoms i, j :

$$\Delta\epsilon_{ij} = \epsilon_{ij} - \epsilon_i - \epsilon_j; \quad (3)$$

similarly, the $\Delta\epsilon_{ijk}$ are non-additive parts of the total energies ϵ_{ijk} of trimers corrected for pair interactions:

$$\Delta\epsilon_{ijk} = \epsilon_{ijk} - (\Delta\epsilon_{ij} + \Delta\epsilon_{ik} + \Delta\epsilon_{jk}) - (\epsilon_i + \epsilon_j + \epsilon_k). \quad (4)$$

Such an expansion has been shown to work very well for vdW crystals like the rare gases⁷. Here, the decay of the contributions is fast enough with distance ($\sim 1/r^6$ in the leading term of the vdW pair interaction), the expansion is dominated by pair contributions making higher

terms almost negligible, and the nature of the interaction changes very little when going from small clusters (dimers, trimers, ...) to the infinite crystal.

It may be argued that it is just the last point which makes this type of expansion less successful for mercury: the metallic solid has not very much in common with the vdW bound small clusters. However, we will see that even for smaller mercury clusters, where we would still expect some vdW like behaviour, the convergence of the many-body expansion is not smooth at smaller distances. An obvious possibility for improvement is to treat the HF part of the total energy separately, i.e., without many-body expansion, in a calculation for the bulk solid like in Sec. II. The many-body expansion for the remaining part of the total energy (the correlation energy) is expected to be both less problematic and more general, since i) electron correlation effects are known to be more local than interactions at the independent-particle level, and ii) the decay of electron-correlation contributions for distant pairs of localized orbitals (or orbital groups) shows a vdW-like behaviour not only in vdW crystals but also in ionic and covalently bonded systems.

Still, localized entities in ionic and covalently bonded solids may be quite different from those in free (neutral) atoms or small clusters. Therefore, it may be vital to base the many-body expansion of the correlation energy on suitable localized orbitals or orbital groups as they appear in the solid (e.g., atoms or ions modified by crystal surroundings, bond orbitals, etc.); the necessary information can be taken directly from solid-state calculations or from calculations for suitably embedded clusters. Such a type of expansion has been successfully applied by our group to a wide range of ionic crystals and semiconductors, cf. e.g.^{21–23}.

A direct transfer of this approach to metallic systems is not possible, however, since localized orbitals become very long-range entities here and a many-body expansion in terms of such orbitals cannot be expected to have useful convergence characteristics. Moreover, it is currently not clear how to treat electron correlation within wave-function based methods for metallic systems, since it becomes highly multi-configurational in nature, and a full CI treatment is not feasible. In order to make the expansion still computationally feasible, we have suggested recently¹⁷ to start from suitable model systems where long-range orbital tails are absent, and to allow for delocalization only successively in the course of the expansion; more specifically, when calculating pair contributions for a given orbital (or orbital group) combination (i, j) , we allow for delocalization $i \rightarrow j$ and $j \rightarrow i$, and similarly with the 3-body terms we allow for delocalization over the triples of atoms, etc. It is clear that the final result is not affected, only the convergence properties of the many-body expansion are changed. As an additional advantage, we can calculate individual terms of the expansion from (suitably modelled/embedded) finite clusters of reasonable size. In the case of mercury, for example, we can force localization of the solid by us-

ing a *s*-type atomic basis set for describing the valence-electron system. This way, delocalization due to *sp*-mixing is avoided, but still each atom has its correct crystal surroundings concerning the van der Waals interaction. When determining a many-body contribution for a given set of atoms, we can use the full basis for this set of atoms and thus successively allow for metallic delocalization.

IV. MANY-BODY INCREMENTS FOR EMBEDDED CLUSTERS

As already mentioned in the previous section, we want to use finite cluster models for embedded *n*-tuples of atoms, in order to calculate individual terms (*n*-body increments) of the many-body expansion of mercury. These cluster models have to meet the following requirements: i) their geometry should reflect the experimental geometry of a suitably chosen section of the Hg crystal, in order to mimic the influence of the bulk surroundings on the *n* inner atoms to be correlated; ii) their electronic structure should simulate that of a hypothetical Hg crystal with the highest occupied band derived from atomic *6s* states only, whose Wannier orbitals are well localized and well transferable, without significant finite-size and surface effects, to the cluster models in question.

According to requirement i), the geometries of the embedded clusters were generated as follows. The rhombohedral structure of the infinite crystal can be viewed as a central atom surrounded by atom shells of various size. The first shell contains 12 atoms, 6 of them at distance a_0 ($=3.005$ Å) and 6 at $1.155 a_0$; the next shells contain 6 atoms at distance $1.528 a_0$, 6 atoms at $1.633 a_0$ another 24 atoms up to a distance of $2 a_0$. This already defines various levels of embedding for a single atom when calculating the one-body term of the many-body expansion. For calculating a two-body term between neighbouring atoms, we include all atoms in the embedding which are in the first shell of one of the two atoms to be correlated. If the two atoms to be correlated are more distant, we additionally select for the embedding all atoms lying within a cylinder of the shell radius around the connection line. Since the number of embedding atoms is large, we do not use here the small-core (20-valence-electron) pseudopotential mentioned in Sec. 2, but rather a 2-valence-electron scalar relativistic pseudopotential²⁴ which simulates the Hg $5s^2 5p^6 5d^{10}$ shells within the atomic core. Thus, only the *6s*, *6p* and higher atomic shells are explicitly treated; truncating the corresponding optimized $(4s4p1d)/[2s2p1d]$ valence basis set to $(4s)/[2s]$, we satisfy requirement ii).

For calculating the individual *n*-body increments in the embedded clusters, we have to treat the orbitals of the *n* atoms involved (which are in the center of the embedded cluster) as accurately as possible. We equip these atoms with the small-core pseudopotential, i.e., we explicitly treat the outer-core *5spd* shells in the valence

space; furthermore, we invoke the (unmodified) primitive $(7s7p6d1f)$, $(10s9p7p2f1g)$, and $(12s12p9d3f2g1h)$ basis sets of Ref.¹⁴. Two different contraction patterns of these primitive basis sets are considered in the following. In the first step of our calculation, the aim is to define the localized orbitals corresponding to the hypothetical mercury mentioned above. Here, we choose contractions which are closely analogous to that for the embedding atoms: the outer-core $5spd$ orbitals and the valence $6s$ orbital are fully contracted using the orbital coefficients of the free atoms, and the most diffuse s function of the primitive sets are added to provide more flexibility within the s space; this leads to a $[3s1p1d]$ set. Since valence p functions are not represented in these basis sets, delocalization of the orbitals is still avoided. Thus, a unitary transformation of the occupied canonical orbitals according to the criterion of Foster and Boys²⁵ yields well localized orbitals on the individual atoms, which can be separated into embedding orbitals and orbitals to be correlated.

In the next step, we improve the description of the atoms to be correlated while keeping frozen the localized orbitals which can be attributed to the atoms of the embedding region. The basis sets of the former atoms are enlarged by successively decontracting the above-mentioned basis sets with respect to the most diffuse exponents. Specifically we consider a $(7s7p6d1f)/[7s6p5d1f]$ set (basis A), a $(10s9p7d2f1g)/[8s7p6d2f1g]$ set (basis B), and a $(12s12p9d3f2g1h)/[9s8p7d3f2g1h]$ set (basis C). Using these basis sets, we recalculate the integrals and reoptimize the orbitals of the atoms to be correlated, in a HF calculation. This provides us with orbitals which are still fairly local but are more or less delocalized over the atoms i, j, \dots to be correlated. Finally, on top of this HF calculation and still keeping frozen the localized orbitals of the embedding region, we introduce electron correlation by performing a coupled-cluster calculation with single and double excitations and perturbative treatment of the triples (CCSD(T)). All these calculations are performed using the MOLPRO suite of ab-initio programs^{26–28}. Note that only the correlation-energy piece, $\epsilon_{i,j,\dots}$, of the last calculation enters the many-body expansion of Sec. III (eqs. 1 - 3).

Test calculations have been performed checking the influence of geometry (number of shells with embedding atoms) and basis-set description of the embedding region on the calculated n -body increments. For the one-body increment we checked clusters with up to 7 shells, for the nearest-neighbour two-body increment clusters with up to 4 shells. All calculated one-body and two-body increments differ by at most by 0.1mHartree, respectively. On the basis of these test calculations and in order to avoid excessive computational effort, we feel justified to restrict embedding to the first shell, for the calculations of the following sections, and to describe the embedding atoms with the large-core pseudopotential and the corresponding $(4s)/[2s]$ basis set.

V. ONE-BODY CONTRIBUTION TO COHESION

It is only for the many-body expansion with embedding that the one-body increment can contribute to the binding. We define the cohesive contribution of the one-body increment as the difference between the correlation energy of the embedded atom ϵ_i and that of the free atom $E_{\text{free}}^{\text{corr}}$.

$$\epsilon_i^{\text{coh}} = \epsilon_i - E_{\text{free}}^{\text{corr}} \quad (5)$$

The free atom is calculated with the same basis as the embedded atom, but in order to minimize basis-set superposition effects we add one shell of ghost atoms (i.e., atoms with zero charge carrying $(4s)/[2s]$ basis sets) at the 12 nearest-neighbour sites of the mercury lattice. The difference between the correlation energy with this basis set and that with the uncontracted basis set of the free atom is less than 1 mHartree.

In Table I, the one-body contribution to the binding is listed for different basis sets, and different number of correlated atomic orbital shells. All contributions are repulsive; the embedded atom has a smaller (absolute) correlation energy than the free atom. This effect is due to the crystal cage effect leading to a more compact $6s^2$ shell but also to increased excitation energies. As can be anticipated the dominant correlation contributions to ϵ_i^{coh} come from the $6s^2$ shell. Intra-shell contributions from the outer-core shells are also repulsive, but significantly smaller; moreover the latter contributions are nearly compensated by the $5d - 6s$ inter-shell correlation which becomes increasingly attractive with increasing compactness of the ‘in-crystal’ atoms. Interestingly, although $5sp - 5d6s$ inter-shell effects are small in magnitude they can be seen to become repulsive again. Finally, basis effects are small: adding diffuse functions (as detailed in Sect. 6), or going from basis set B to C changes the total ϵ_i^{coh} by not more than 0.1 mHartree.

VI. TWO-BODY CONTRIBUTIONS

In a first step, we checked our basis sets for the free dimer where experimental values and data from accurate calculations are available in literature^{12–14}. Since the vdW binding is very weak (of the order of 1 mHartree) and relies on an accurate description of the orbital tails, we added diffuse functions to our basis sets; more specifically, one diffuse function for each l value was added in an even-tempered way (the resulting basis sets being designated as augA, augB, augC). In Fig.1, the Hg_2 potential curve is plotted for basis sets B, augB, and augC, for various choices of the active space of correlated orbitals; all curves contain counterpoise corrections²⁹ for (approximately) removing basis-set superposition errors. The HF curve is purely repulsive. Correlating the $6s^2$ shell leads to binding, but the dissociation energy D_e is too small by more than a factor of 3, with respect to the experimental

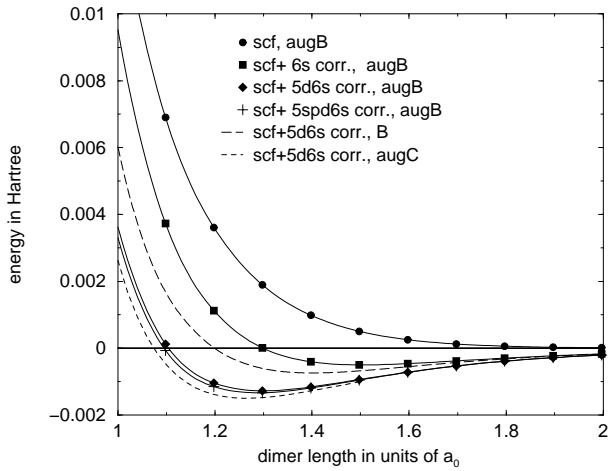


FIG. 1. The potential curve of the Hg dimer is plotted for different basis sets (B, augB, augC) at the Hartree-Fock (scf) and correlated levels (corr.). In the latter case, the active space of correlated orbitals is indicated (6s, 5d6s, 5spd6s). $a_0 = 3.005 \text{ \AA}$

active space	augC	augB	B
$6s^2$	+0.004154	+0.004155	+0.004230
$5d^{10}6s^2$	+0.004436	+0.004582	+0.004260
$5s^2p^6d^{10}6s^2$	+0.005041	+0.005104	+0.005089

TABLE I. The one-body contribution to the cohesive energy $\epsilon_i - E_{\text{corr}}^{\text{free}}$ of embedded clusters (in Hartree) is calculated at the CCSD(T) level with different basis sets (B, augB, augC), and different active spaces included in the correlation treatment. For more details, cf. text.

value, and the bond length R_e is too long by more than 0.6 Å. Only with correlating the outer-core $5d^{10}$ shell is it possible to obtain reasonable results; the influence of the underlying $5s^25p^6$ shells, on the other hand, is only marginal. More important than the latter correlation effect is the role of the basis set; especially prominent is the role of the diffuse functions, as shown by comparing the B and augB curves: D_e is enhanced by nearly a factor of 2, R_e is shortened by ~ 0.3 Å; going from basis augB to augC leads to further improvement and yields the following values for the spectroscopic constants (experimental values in parentheses): 3.80 (3.69 \pm 0.01) Å for R_e , 17.9 (19.6 \pm 0.3) cm $^{-1}$ for the harmonic wavenumber ω_e , and 328 (380 \pm 15) cm $^{-1}$ for D_e .

We now use the above free-dimer data for the many-body expansion of solid mercury. The relevant increments are given in Table IV. It is seen that for the nearest-neighbour increment ($d = a_0$) d -shell correlation enhances the valence ($6s^2$) correlation effect by more than a factor of 2, but this factor gradually diminishes to $\sim 10 - 20\%$ for $d = 1.9a_0$. The inclusion of diffuse basis functions is important; the $\Delta\epsilon_{ij}$ become more attractive

by 20 - 30 % when going from basis set B to augB (and by another 5 - 10 % when going from aug-B to augC). While all correlation-energy increments are attractive, the nearest-neighbour increment becomes repulsive when including the Hartree-Fock energy into the many-body expansion. Since the Hartree-Fock closed-shell Pauli repulsion is a short-range effect, already the 2nd-nearest-neighbour increment $d = 1.15a_0$ remains slightly attractive, and the increments with $d > 1.6a_0$ are hardly affected at all.

Correlation-energy increments $\Delta\epsilon_{ij}$ for embedded clusters are also listed in Table IV, again for different basis sets (B, augB, augC) and correlated active spaces ($6s^2$, $5d^{10}6s^2$). The basis-set dependence turns out to be roughly the same as for the free dimers (except for the fact that the diffuse functions are less important because they are already simulated by the basis sets of the embedding atoms). However, the nearest-neighbour increment is larger by $\sim 15\%$ as compared to the free-dimer case, while changes into the opposite direction occur for the increments between more distant atoms. These findings may be rationalized in terms of the crystal cage effect leading to an increased overlap between nearest neighbours (the embedding forcing the electrons to stay nearer to the atoms and to the bond between them) but a reduced 'in-crystal' polarizability of the atomic entities. Again, the contribution of the outer-core $5d$ shell is very important for the nearest-neighbour increment. As for the free dimers, the overall decay of the increments with distance is fairly rapid. Moreover, from a distance around $1.5a_0$ on the basis set effects are very small on an absolute scale and hence can be neglected; there, basis set B is sufficient. For basis B, we have performed the calculation of the 2-body increments up to a distance of $3.0 a_0$, where the increment is less than $10 \mu\text{Hartree}$. We have fitted a vdW expression to the increments of the region from $1.5 a_0$ to $2.8 a_0$. The resulting value for C_6 , 297 atomic units, is comparable with data from the literature^{13,30,31} where the van der Waals constant for the free dimer was determined.

VII. THREE-BODY CONTRIBUTIONS

As found by Schwerdtfeger and co-workers¹⁵, three-body terms are very important for mercury clusters and solid mercury, especially the short-range contributions. We have calculated, therefore, all 3-body increments where at least 2 distances are within the first-neighbour shell (i.e., smaller than $1.16 a_0$), using basis sets B and augB. The results are given in Table V.

For the free trimers, the largest contributions arise for the compact geometries; for the simplest type of many-body expansion (total-energy expansion), these contributions are of the same magnitude as the largest two-body increments; since the number of 3-body increments (including weight factors) is larger than that of the two-

body ones, the two-body repulsion is thus overcompensated by three-body attraction. The three-body attraction for Hg_n clusters is in sharp contrast to the rare gas elements, which has the consequence that the Hg_3 distance becomes shorter compared to Hg_2 ¹⁵.

The situation is different when the many-body expansion is performed for the correlation energy only. Here, the two-body terms are attractive, and this attraction is weakened by (mostly repulsive) three-body increments; the ratio of the largest two-body and three-body increments, respectively, is $\sim 6:1$. The largest three-body increments still arise for compact geometries, and are by a factor of 2 smaller than in the total-energy case. The basis-set dependence turns out to be less critical for the three-body increments than for the two-body ones: adding diffuse functions to basis set B ($B \rightarrow \text{aug}B$) changes the individual increments by mostly less than 0.1 mHartree. Thus, we decided to leave out the diffuse functions for the embedded clusters; here, the role of the latter functions is simulated by the basis sets of the embedding atoms, leading to a reduced basis-set dependency already for the two-body increments (cf. Table IV).

Looking at the results for the embedded trimers now, we see that the convergence behaviour of the many-body expansion is significantly improved once more: the largest three-body correlation-energy increment is 4 times smaller than for the free-trimer case, and ~ 20 times smaller than the largest (embedded) two-body increment. The embedded three-body terms are mostly attractive (i.e., of the same sign as the embedded two-body terms); valence ($6s^2$) correlation dominates, except in cases where at least one distance of the (embedded) trimer is the shortest possible (nearest-neighbour) one – there, $6s - 5d$ inter-shell correlation is of a magnitude nearly comparable to that of $6s^2$ correlation. For the nearly equidistant triangle the $5d$ correlation is attractive, but for the linear arrangement of 3 atoms it is repulsive. This behaviour can be rationalized in terms of the Axilrod-Teller dipole-dipole-dipole interaction³². The valence-only values show just the reverse dependence on the angle. By far the largest (total) contribution (-0.4 mHartree) is the attractive one for the linear arrangement; this might be connected to the fact that static polarization of the central atom is suppressed there and is (partially) compensated by correlation. For the linear trimer, we checked the basis-set dependency: going from basis set B to C changes the increment from -0.4 to -0.5 mHartree.

VIII. FOUR- AND HIGHER BODY CONTRIBUTIONS

For the four-body contributions, we selected 5 compact geometries, the tetrahedron-like one, a linear one, and three planar geometries (a rhombus, and two geometries

	free scf+ $5d^{10}6s^2$	$5d^{10}6s^2$	embedded $5d^{10}6s^2$
tetrahedral-like	+6588.4	-2373.3	-5.9
planar, Y-like	+742.8	-726.4	+107.6
planar, L-like	-73.5	-40.3	+93.0
linear	+321.8	-54.3	+170.1
planar,rhombus	-1090.7	-820.4	-20.0

TABLE II. The four-body increments, $\Delta\epsilon_{ijkl}$ (in μ Hartree) for compact 4-atom clusters of the rhombohedral structure are calculated at the CCSD(T) level with basis A. For the free and embedded clusters the correlation-energy increments for the $5d^{10}6s^2$ active space are listed, for the free clusters also the total-energy contribution is given.

with 3 atoms in line and the fourth one connected to the first atom (L-like) or to the middle atom (Y-like)). The results are listed in Table II. They were obtained without diffuse functions, and basis set A was used instead of B in order to reduce the computational effort. We checked, however, for the linear geometry that basis B would change this increment by just about 20%. For the embedded case, the increments are smaller in magnitude than the 3-body terms, their sum is repulsive. The linear geometry has the largest contribution (0.2 mHartree). This is totally different for the free tetramers: As for the corresponding 3-body terms, the compact ones yield the largest absolute contribution both at the HF and the correlated level (6.6 mHartree in total, -2.4 mHartree for the correlation piece). Considering the magnitude of the four-body increments, we see that the values do not decrease with respect to those for the trimers. Thus, the convergence of a many-body expansion based on non-embedded Hg clusters appears to be questionable, even if it is done for the correlation energy only.

To make this point even more transparent, we calculated all n -body contributions up to $n=6$ for octahedral Hg_6 . Since coupled cluster calculations are computationally too demanding for this size, we carried out second-order many-body perturbation theory (MBPT2) calculations for the correlation energy using a somewhat reduced correlation consistent ($6s5p4d1f$)/[$4s4p3d1f$] basis set (basis D) which minimizes the basis set superposition error (BSSE). The n -body contributions are shown in Fig.2 as a function of the Hg-Hg distance in Hg_6 kept in O_h symmetry. At short bond distances (3.0 Å) the two-body part becomes repulsive as expected. However the 3-body part remains attractive, giving -343% of the total (non-binding) energy in contrast to the +274% due to the 2-body interaction. The higher body terms contribute 183%, -123%, and 109% for the 4-, 5-, and 6-body contributions respectively (a negative sign indicates binding here where the total energy is positive in contrast to the case below). At such short distances the HOMO/LUMO gap is still

large. Hence, the bad convergence of the many-body expansion is not directly related to the change to the

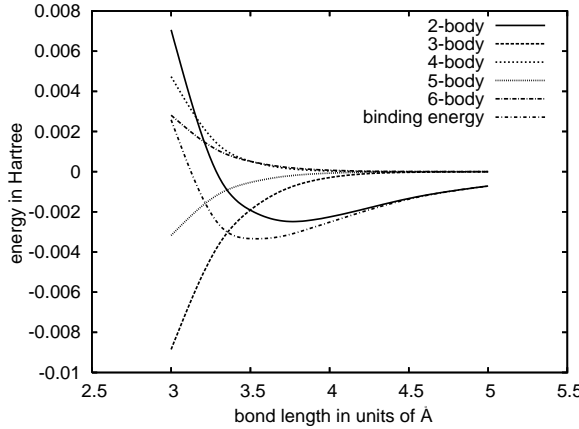


FIG. 2. Individual 2-, 3-, 4-, 5- and 6-body contributions (in Hartree) to the dissociation energy per atom for Hg_6 at different Hg-Hg bond distances.

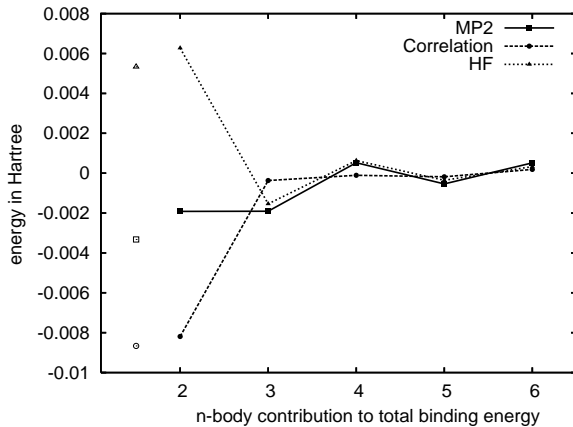


FIG. 3. Individual 2-, 3-, 4-, 5- and 6-body contributions (in Hartree) to the dissociation energy per atom for Hg_6 at the equilibrium MBPT2 geometry. The disconnected symbols are the total energy contributions summed over all n-body interactions.

metallic state. Above 3 Å the 2-body part becomes attractive, and the contributions of each many-body term relative to the binding energy of the 6-atom cluster decrease. While at short distances the 3-body term is the contribution of highest magnitude, above 3.5 Å the 2-body term becomes increasingly more important. However even at 4 Å the 3-body term accounts for +12% of the binding energy, followed by 4-, 5-, and 6-body contributions of -1.4%, 2.9%, and -2.9%. While these contributions are not entirely negligible, it is clear that at longer distances the many-body expansion begins to converge. According to an earlier study we expect mostly vdW behaviour at distances down to 5 Å²⁰. Hence, the bad convergence of the many-body expansion is related to the fact that the bond distance shortens dramatically from the more vdW type system of Hg_2 (3.69 Å) to the solid state (3.0 Å).

We also investigated the convergence behaviour of the energy needed to remove one Hg atom from the cluster, which in the high n limit also converges towards the cohesive energy. Again, we do not see a great improvement in the convergence behaviour of the n -body expansion.

Fig. 3 shows the HF, correlation and total n -body contributions for Hg_6 at the optimized MBPT2 equilibrium distance of 3.499 Å. The oscillating behaviour of the n -body terms is clearly seen. The 2- and 3-body contributions are almost exactly equal, 58% and 57% of the total binding energy. The 4-, 5-, and 6-body contributions are all important at -16%, +16% and -15% respectively. Fig. 3 also shows the sum over all n -body contributions (detached symbols shown at left), which demonstrates that while the n -body expansion is starting to converge, the higher n -body contributions are still not negligible at this size. Hence, the expansion shown in eq.1 is of limited use for the total energy of free clusters. However, the correlation energy shows a much better convergence behavior at 3.499 Å, Fig. 3. Even at 3.0 Å the 2-body correlation energy is the major term with 94.3%, the higher-order terms becoming much smaller with the 3-body 2.0%, the 4-body 4.7%, the 5-body 1.2%, and the 6-body -2.3%. Obviously, this explains the nice convergence behavior in the solid state calculations for the correlation part.

IX. RESULTS FOR THE COHESIVE ENERGY OF BULK MERCURY

In Table III we list the various contributions to the cohesive energy of solid mercury applying different types of many-body expansion. Looking first at results for the many-body expansion of the correlation energy derived from embedded-cluster data, we see that the 2-body term is the dominant one, the 3-body contribution of the first shell being smaller by a factor of 5. There is a further decrease by about a factor of 3 when going to the 3-body terms of the second shell or to the most important 4-body terms. Summing up all contributions calculated

	CRY emb	CRY free	MB free
HF	+36.2	+36.2	
1-body, basis B	+4.2		
1-body, basis augB	+4.6		
1-body, basis augC	+4.4		
2-body, basis B	-50.0	-44.7	+12.7
2-body, basis augB	-57.5*	-56.7	-0.1
2-body, basis augC	-61.2*	-61.3	-4.8
3-body(1st), basis B	-9.2	+20.0	-39.5
3-body(1st), basis augB	—	+19.1	-40.4
3-body(2nd), basis B	-2.4	+2.8	-2.9
3-body(2nd), basis augB	—	+0.8	-4.0
4-body, basis A	+3.0	-16.6	+18.9
total, best available basis	-29.2	-21.8	-30.3

TABLE III. Contributions to the cohesive energy of solid mercury (in mHartree) are listed for different many-body expansions (including the Hartree-Fock energy in the many-body expansion (MB) or using the crystal HF energy (CRY), calculating the correlation energy increments from free (free) or embedded clusters (emb)) and different basis sets (A, B, augB, augC). For the 1-body term the contribution of the free atom is subtracted. The 2-body increments are summed up to a distance of $2.52 a_0$. (For the augmented basis sets, the * means that only increments up to a distance of $1.92 a_0$ are calculated with the basis set indicated, while basis set B is used for the rest.) The sum of the 3-body increments for the first shell is taken over the increments with 2 distances smaller $1.16 a_0$, for the second shell over increments with 2 distances smaller than $1.63 a_0$. The 4-body contributions is the sum over 5 compact clusters. The experimental value is -29 mHartree¹¹.

with the largest available basis set (Table III) we obtain -29.2 mHartree. The cohesive energy is therefore 0.79 eV, in very good agreement with the experimental value. But the approximations applied, especially the finite one-particle basis set and the neglect of further 4-body terms yield an error bar of about 10% for the calculated value of the cohesive energy.

Replacing the many-body expansion for the correlation energy of the embedded clusters by a corresponding expansion for free clusters, leads only to a moderate decrease of the (absolute value of the) binding energy. However, the 3-body and 4-body terms are of comparable magnitude (and of the same order of magnitude as the experimental cohesive energy) indicating that the result is not properly converged. Similar convergence problems are encountered with a many-body expansion of the total energy (HF + correlation) for free Hg clusters. Again, the sum of the increments considered in this paper would lead to more or less reasonable results, but the 3-body contribution is now more than three times larger than the 2-body one (while the factor was about 1/3 for the correlation-only many-body expansion for free clusters). Thus, the many-body correlation-energy expansion for embedded clusters is found to provide more reliable results. It is to be seen how well this new type of expansion, which has been applied to metals for the first time in the present and a companion¹⁷ paper, works for other properties of mercury like lattice constants and the bulk modulus.

X. CONCLUSIONS AND OUTLOOK

We have demonstrated that the cohesive energy of mercury can be obtained with good accuracy from solid state HF calculations adding n -body correlation calculations for embedded mercury clusters. However, the simulation of free mercury clusters where surface effects are dominant will represent a considerable challenge for future quantum theoretical investigations. First, the n -body expansion only converges for free clusters above a critical bond-length where van der Waals bonding becomes dominant. The bad convergence of the n -body expansion for mercury can subsequently lead to a bad convergence of the vdW equation which contains the well known virial coefficients. Hence, the accurate simulation of gaseous or liquid mercury is currently a formidable task. Second, DFT does not produce reliable results for such clusters and an improvement for describing both low and high n limits is required, that is the vdW system for smaller clusters, and metallic state for the solid. Third, single-reference wavefunction based methods such as CCSD(T) will fail as the cluster becomes closer to the metallic state with increasing size. A possible way out of this dilemma can be a multi-reference incremental scheme, as it was successfully applied for the one-dimensional model system lithium³³. Combining this method with the embed-

ding proposed here for metallic systems could provide a quantum chemical method for metals like barium, where the metallicity is stronger than in mercury.

ACKNOWLEDGEMENTS

Support by the Marsden Fund (Wellington) is gratefully acknowledged. N. G. acknowledges support from FRST (Wellington).

Preuss, *Theor. Chim. Acta* **77**, 123 (1990). (The *f* and *g* projectors are omitted in the Crystal code.)

²⁰ P. Schwerdtfeger, J. Li, and P. Pyykkö, *Theor. Chim. Acta* **87**, 313 (1994).

²¹ H. Stoll, *Phys. Rev. B* **46** (1992) 6700.

²² B. Paulus, P. Fulde and H. Stoll, *Phys. Rev. B* **54** (1996) 2556.

²³ K. Doll, M. Dolg, P. Fulde and H. Stoll, *Phys. Rev. B* **52** (1995) 4842.

²⁴ W. Küchle, M. Dolg, H. Stoll, and H. Preuss, *Mol. Phys.* **74**, 1245 (1991).

²⁵ J.M. Foster and S.F. Boys, *Rev. Mod. Phys.* **32**, 296 (1960).

²⁶ MOLPRO version 2002.6 - a package of *ab-initio* programs written by H.-J. Werner and P. J. Knowles with contributions from J. Almlöf, R. D. Amos, A. Bernhardsson, A. Berning, P. Celani, D.L. Cooper, M. J. O. Deegan, A.J. Dobbyn, F. Eckert, C. Hampel, G. Hetzer, T. Korona, R. Lindh, A.W. Lloyd, S.J. McNicholas, F.R. Manby, W. Meyer, M.E. Mura, A. Nicklass, P. Palmieri, R. Pitzer, G. Rauhut, M. Schütz, H. Stoll, A.J. Stone, R. Tarroni, and T. Thorsteinsson.

²⁷ C. Hampel, K. Peterson, and H.-J. Werner, *Chem. Phys. Lett.* **190** (1992) 1.

²⁸ M. J. O. Deegan and P. J. Knowles, *Chem. Phys. Lett.* **227** (1994) 321.

²⁹ S.F. Boys and F. Bernardi, *Mol. Phys.* **19** 553 (1970).

³⁰ B. Hartke, H.-J. Flad and M. Dolg, *Phys. Chem. Chem. Phys.* **3**, 5121 (2001).

³¹ C. F. Kunz, C. Hättig, B. A. Hess, *Mol. Phys.* **89**, 139 (1996).

³² B. M. Axilrod and E. Teller, *J. Chem. Phys.* **11**, 299 (1943).

³³ B. Paulus, *Chem. Phys. Lett.* **371** (2003) 7.

d_{ij}/a_0	free				embedded				B
	scf+5d ¹⁰ 6s ²		6s ²		5d ¹⁰ 6s ²		5d ¹⁰ 6s ²		
	augC	augB	augC	augC	augB	augC	augC	augB	
1.000	+2579	+3619	-4030	-10759	-9805	-4592	-12033	-11243	-9842
1.16	-1140	-701	-2858	-5909	-5476	-2706	-5636	-5310	-4545
1.53	-927	-867	-935	-1336	-1281	-594	-928	-891	-754
1.63	-679	-643	-652	-878	-844	-462	-674	-650	-563
1.92	-277	-266	-248	-303	-292	-236	-285	-274	-210

TABLE IV. The two-body increments $\Delta\epsilon_{ij}$ (in μ Hartree) for different distances d_{ij} occurring in the rhombohedral structure are calculated for the free and embedded dimers at the CCSD(T) level using different active spaces of correlated orbitals ($6s^2$, $5d^{10}6s^2$) and different basis sets (B, augB, augC). The values in the columns ‘scf+5d¹⁰6s²’, include the Hartree-Fock energy within the many-body expansion, cf. Sect. 3.

d_{12}	d_{13}	d_{23}	free			embedded			B
			scf+5d ¹⁰ 6s ²	augB	5d ¹⁰ 6s ²	6s ²	5d ¹⁰ 6s ²	B	
1.00	1.00	1.16	-3012.8	+1704.1	+1608.6	+83.4	-91.5		
1.00	1.00	1.63	-914.6	+423.5	+460.4	-209.9	-329.0		
1.00	1.00	2.00	-174.2	-419.9	-249.6	-579.4	-423.2		
1.00	1.16	1.53	-696.7	+586.1	+568.9	-359.5	-124.4		
1.00	1.16	1.92	-302.7	-46.3	+7.5	-206.7	-245.7		
1.16	1.16	1.16	-1264.7	+1035.2	+973.0	+86.6	+94.3		
1.16	1.16	2.00	-163.7	-21.7	+3.7	-102.7	-125.9		
1.16	1.16	2.31	-147.3	-239.7	-185.8	-179.2	-151.4		

TABLE V. The three-body increments $\Delta\epsilon_{ijk}$ (in μ Hartree) for compact 3-atom clusters of the rhombohedral structure are calculated at the CCSD(T) level with different basis sets (B and augB), and different correlated orbital spaces ($6s^2$, $5d^{10}6s^2$). The d_{ij} are interatomic distances (in units of a_0). Results are given for trimers with and without embedding (embedded, free). The values in the column ‘scf+5d¹⁰6s²’ include the Hartree-Fock energy within the many-body expansion, cf. Sect. 3.